

CrossMark  
click for updatesCite this: *J. Mater. Chem. A*, 2017, 5, 1948Received 2nd November 2016  
Accepted 22nd December 2016

DOI: 10.1039/c6ta09469d

www.rsc.org/MaterialsA

## Introduction of metal precursors by electrodeposition for the *in situ* growth of metal–organic framework membranes on porous metal substrates†

Sheng Zhou, Yanying Wei,\* Libin Zhuang, Liang-Xin Ding and Haihui Wang\*

We report here a facile and efficient electrodeposition method to modify inexpensive porous stainless-steel nets for use as substrates in the *in situ* growth of metal–organic framework membranes, such as ZIF-8, ZIF-67 and HKUST-1. Using this method, different metal precursors can be electrodeposited depending on the central metals required in the target metal–organic frameworks. The inorganic modifiers prepared by this approach are sufficiently reactive for the one-step growth of continuous metal–organic framework membranes; their reactivity is comparable with that of organic functional groups. The procedure is also green and cost-effective, which is promising for use in large-scale production.

Membrane separation is a promising technology for industrial-scale separation and purification processes as a result of its low consumption of energy.<sup>1</sup> Metal–organic frameworks (MOFs) have great potential for use as membranes in separation processes because their pore size can be tuned and they have highly designable structures and adsorption properties.<sup>2</sup> The preparation of supported MOF membranes has attracted increasing attention in separation technology.<sup>3</sup> Shekha *et al.*<sup>4</sup> used a stepwise layer-by-layer (LBL) growth method to prepare MOF thin films of HKUST-1 and zeolitic imidazolate framework 8 (ZIF-8) directly on confined surfaces and demonstrated the potential of the LBL method in the controlled growth of MOF thin films on different substrates. They also developed a liquid phase epitaxy method for the construction of oriented ZIF-8 thin films on functionalized surfaces<sup>5</sup> and paved the way for the preparation of ZIF-8 thin films on porous substrates. They also succeeded in preparing ultra-thin and defect-free ZIF-8 membranes on porous supports for use in gas separation.<sup>6</sup>

Although various methods have been used to fabricate MOF membranes, it is still challenging to build a versatile platform

for the *in situ* growth of MOF membranes.<sup>7</sup> There have been many reports on the modification of substrates with organic functional groups prior to the *in situ* growth of MOF membranes. Caro and coworkers used 3-aminopropyltriethoxysilane as a covalent linker to grow a series of ZIF membranes (ZIF-22,<sup>8</sup> ZIF-90 (ref. 9) and ZIF-95 (ref. 10)). Polydopamine was shown to be powerful and effective for the fabrication of MOF membranes, including ZIF-8,<sup>11</sup> ZIF-90 (ref. 11) and ZIF-100.<sup>12</sup> Many other organic compounds, such as polyethyleneimine,<sup>13</sup> poly(methyl methacrylate)<sup>14</sup> and polyaniline<sup>15</sup> have been used as reactive linkers to modify substrates.

Inorganic modifiers are more environmentally friendly than organic modifiers, however. Qiu and coworkers prepared Ni-based and Cu-based MOF membranes on nickel nets<sup>16</sup> and copper nets<sup>17</sup> *via* a twin copper source method. Neelakanda *et al.*<sup>18</sup> used a double zinc source method to manufacture ZIF-8 membranes on a polymeric substrate. Zhang *et al.*<sup>19</sup> grew ZIF-8 membranes on ZnO nanorod modified supports *via* a hydrothermal method. Liu *et al.*<sup>20</sup> used Zn-based layered double hydroxide buffer layers as surface modifiers to provide active sites for the nucleation of Zn-based MOF crystals for membrane growth.

There are still some challenges in the development of inorganic modifiers, however, which urgently need to be overcome. The traditional methods for the introduction of inorganic modifiers, such as calcination<sup>21</sup> or hydrothermal treatment, are both complicated and time consuming.<sup>19,20</sup> In addition, the inorganic compounds currently used as modifiers are not as reactive as organic modifiers, which makes it difficult to form continuous MOF membranes.<sup>19</sup> Only one kind of inorganic modifier can be used for metal-based MOF membrane growth, resulting in a lack of versatility and commonality. Therefore it is desirable to develop a simple and universal strategy to prepare inorganic surface modifiers with excellent reactivity for use in different kinds of metal-based MOF membranes.

Inspired by electrochemical applications, we developed a novel electrodeposition-assisted strategy to modify substrates to give a versatile platform for the *in situ* growth of various MOF

School of Chemistry & Chemical Engineering, South China University of Technology, No. 381 Wushan Road, Guangzhou 510640, China. E-mail: ceyywei@scut.edu.cn; hhwang@scut.edu.cn

† Electronic supplementary information (ESI) available: Experimental procedures, characterization data. See DOI: 10.1039/c6ta09469d

membranes. Electrodeposition has attracted much attention in the application of electrochemistry.<sup>22</sup> As a result of the wide range of metals available and the accelerated rate of formation of the metal precursors by the addition of a small current, electrodeposition can be used as a facile and effective method of preparing various metal oxides/hydroxides on conductive substrates.<sup>22</sup> We chose stainless-steel nets (SSNs) as the substrate as they are inexpensive and easily welded. The preparation concept is shown schematically in Fig. 1. A metal oxide/hydroxide with a morphology exactly corresponding to the metal centres of the targeted MOFs is introduced onto the SSN *via* electrodeposition. For example, ZnO nanorods, Co(OH)<sub>2</sub> nanosheets and Cu<sub>2</sub>O nanocubes can be electrodeposited onto substrates quickly and provide active sites for the crystallization of Zn-ZIF-8, Co-ZIF-67 and Cu-HKUST-1, followed by *in situ* growth to form continuous MOF membranes.

The SSN substrate had a uniform pore size of 30 × 6 μm, the microstructure of which is shown in Fig. 2a. The SSN modified by ZnO nanorods was prepared by immersing the pre-cleaned SSN into an aqueous mixture containing Zn(NO<sub>3</sub>)<sub>2</sub>·6H<sub>2</sub>O and NH<sub>4</sub>NO<sub>3</sub> (see ESI†). With the application of a constant current, the concentration of OH<sup>-</sup> near the SSN increased due to the electrolysis of water (eqn (1)) and the precursor of Zn(OH)<sub>2</sub> was initially formed on the substrates as in eqn (2). As a result of the low stability of Zn(OH)<sub>2</sub> under these conditions, it transformed to ZnO through the dehydration reaction in eqn (3). Fig. 2c shows that the ZnO nanorods were closely aligned on the surface of the SSN fibres. The pure phase of ZnO was confirmed by XRD (Fig. S1†). The whole process was environmentally friendly and uniform modification was complete within 90 min.

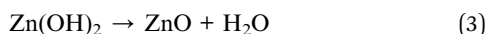


Fig. 1 Schematic illustration of the *in situ* growth of three different MOF membranes on supports modified by electrodeposition.



Fig. 2 Microstructure images of (a) bare stainless-steel nets and (b) ZnO nanorods electrodeposited on stainless-steel nets; (c) high magnification view of ZnO nanorods; (d) top view of as-prepared ZIF-8 membrane; (e) cross-sectional images of ZIF-8 membrane; and (f and g) cross-sectional EDXS mapping images of ZIF-8 membrane.

The ZnO nanorods prepared by electrodeposition had a reactivity comparable with that of commonly used organic modifiers. Thus the SSN modified with ZnO nanorods was used directly for the *in situ* growth of ZIF-8 membranes. Fig. 2d and e show that there were no defects or pinholes in the top view and cross-sectional images.

Zhang *et al.*<sup>19</sup> have previously reported the preparation of ZIF-8 membranes on substrates modified with ZnO nanorods, but the ZnO grown by a seeding procedure under hydrothermal conditions was not sufficiently reactive and required an additional step of activation to create nucleation sites on the surface of the ZnO nanorods. No pre-activation treatment was required for the ZnO nanorods in our study and well-intergrown ZIF-8 membranes were obtained in only one step within 10 h. The enhancement in the reactivity of the ZnO nanorods can be explained by the low synthesis temperature and the presence of intrinsic defects in the ZnO nanorods arising from the electrodeposition strategy.

The proposed *in situ* growth process of ZIF-8 membranes is shown schematically in Fig. 3. The ZnO nanorods served as

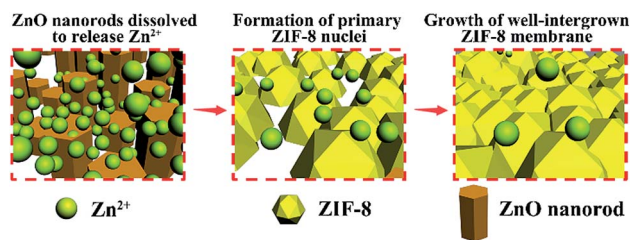


Fig. 3 Schematic illustration of proposed process for the *in situ* growth of the ZIF-8 membrane.

sacrificial precursors for the *in situ* nucleation of ZIF-8 crystals because the ZnO nanorods ultimately disappeared, as shown in the membrane cross-section image (Fig. 2e) and XRD patterns (Fig. S1†). At the initial stage, the ZnO nanorods, as amphoteric oxides, dissolved and released  $\text{Zn}^{2+}$  in the weak alkaline reaction system.  $\text{Zn}^{2+}$  and 2-methylimidazole then coordinated immediately and anchored on the SSN substrates by forming ZIF-8. It is crucial to balance the reaction rates between the two processes of  $\text{Zn}^{2+}$  release from ZnO nanorods and  $\text{Zn}^{2+}$  consumption during the formation of ZIF-8, otherwise the mismatched reaction rates block the *in situ* crystallization of ZIF-8 nuclei on the surface of the substrates. The ZIF-8 crystals at the position of the ZnO nanorods can be regarded as “*in situ* seeds” because they behave as nucleation sites for the subsequent intergrowth of dense ZIF-8 membranes. The final XRD patterns of the ZIF-8 membrane (Fig. S1†) matched well with the simulated ZIF-8 crystals, indicating the successful synthesis of pure phase membranes. By contrast, when unmodified bare SSNs were used, only loosely distributed ZIF-8 crystals were grown on the SSN substrates (Fig. S2†), which demonstrates the requirement for, and advantages of, modification with the ZnO nanorods.

The gas separation performance of the as-synthesized ZIF-8 membrane is shown in Fig. 4. For a 1 : 1 binary gas mixture as a feed gas at 70 °C and 1 bar, the permeation of  $\text{H}_2$  was  $1.1 \times 10^{-7} \text{ mol m}^{-2} \text{ s}^{-1} \text{ Pa}^{-1}$ , much higher than that of other gases such as  $\text{CO}_2$ ,  $\text{N}_2$  and  $\text{CH}_4$ , and a clear cut-off was seen.  $\text{CH}_4$

molecules, with a kinetics diameter (0.38 nm) larger than the pore size of ZIF-8 (0.34 nm), could also pass through the membranes due to the flexibility of the framework.<sup>23</sup> Thus the separation factors of the  $\text{H}_2/\text{CO}_2$ ,  $\text{H}_2/\text{N}_2$  and  $\text{H}_2/\text{CH}_4$  gas pairs were 8.1, 9.6 and 13.6, respectively, much higher than their corresponding Knudsen coefficients and comparable with those of many other ZIF-8 membranes (Table S1†).<sup>24</sup> The ZIF-8 membrane also showed excellent stability during long-term operation, even after series changes in temperature (Fig. 4b).

To check the general application of the strategy by electrodeposition modification, another two MOF membranes with different metal centres, including Co-ZIF-67 and Cu-HKUST-1, were also successfully fabricated using a similar route. The performance of both membranes were tested in the separation of different gases.

For the preparation of ZIF-67 membranes, flower-like  $\text{Co}(\text{OH})_2$  nanosheets were first introduced onto the SSNs by electrodeposition within 40 minutes (Fig. S3b†). In contrast with the full self-sacrifice of ZnO nanorods during ZIF-8 membrane growth, the  $\text{Co}(\text{OH})_2$  nanosheets were not completely consumed (Fig. S3e†). There was still a visible layer of  $\text{Co}(\text{OH})_2$  with a thickness of around 3  $\mu\text{m}$  between the substrate and the ZIF-67 membrane. The existence of  $\text{Co}(\text{OH})_2$  buffer layer was confirmed by energy-dispersive X-ray spectroscopy (EDXS) of the cross-section of the ZIF-67 membrane, where O was only distributed in the intermediate buffer layer and N was only distributed in the upper layer of ZIF-67 (Fig. S3f†). However, the modifier was still highly reactive and the *in situ* growth of the ZIF-67 membrane was completed in one step without any activation treatment. The XRD patterns in Fig. S4† further confirm the formation of the ZIF-67 phase. The ZIF-67 membrane showed an excellent gas separation performance and the ideal separation factors of  $\text{H}_2/\text{CO}_2$ ,  $\text{H}_2/\text{N}_2$  and  $\text{H}_2/\text{CH}_4$  were 8.2, 9.0 and 12.4, respectively, at room temperature (Fig. S5†).

For the preparation of the HKUST-1 membrane with a central  $\text{Cu}^{2+}$ , the electrodeposited metal precursor of  $\text{Cu}_2\text{O}$  in a different valence state also assisted the *in situ* growth of the HKUST-1 membrane. The microstructure of the electrodeposited  $\text{Cu}_2\text{O}$

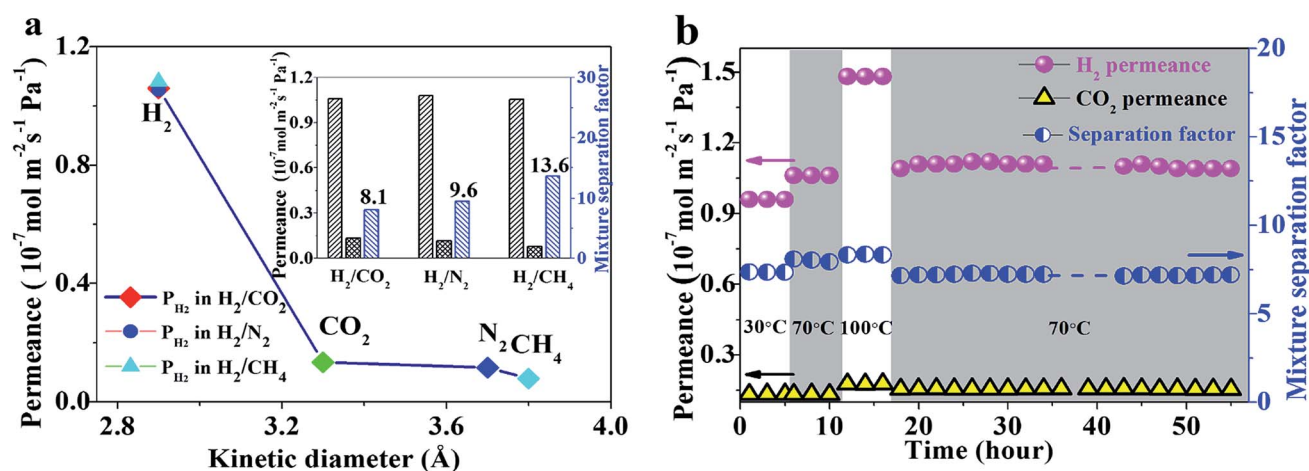


Fig. 4 (a) Mixed gas permeances of different gases through the ZIF-8 membrane prepared on ZnO-modified SSNs at 70 °C as a function of kinetic diameter. The inset shows the mixture separation factors. (b) Stability test of ZIF-8 membranes for  $\text{H}_2/\text{CO}_2$  binary gases.

nanocubes is shown in Fig. S6b† and the pure phase was confirmed by XRD (Fig. S7†). The SEM images in Fig. S6† show the successful formation of the HKUST-1 membrane after *in situ* growth and the pure phase was also confirmed by XRD (Fig. S7†). The as-prepared HKUST-1 membrane was tested for gas separation and an ideal separation factor of 9.7 for H<sub>2</sub>/CO<sub>2</sub> was obtained, indicating that the membrane was intact and well grown (Fig. S8†).

## Conclusions

An efficient electrodeposition strategy is proposed for the introduction of diverse metal clusters into inexpensive SSN substrates. These metal clusters universally act as inorganic modifiers for the subsequent facile *in situ* growth of the MOF membranes. The fast and mild process of modification assisted by electrodeposition is promising for scaled-up production as well as low-cost manufacturing. The excellent reactivity of these metal oxide/hydroxide precursors arising from electrodeposition plays a vital part in the one-step *in situ* synthesis of various MOF membranes. The proposed electrodeposition-assisted strategy simplifies the procedure and can be applied to the preparation of different kinds of metal-centred MOF membranes.

## Acknowledgements

We gratefully acknowledge the funding from the Natural Science Foundation of China for Distinguished Young Scholars of China (no. 21225625), the Natural Science Foundation of China (21536005, 51621001) and the Natural Science Foundation of the Guangdong Province (2014A030312007).

## Notes and references

- 1 N. W. Ockwig and T. M. Nenoff, *Chem. Rev.*, 2007, **107**, 4078.
- 2 (a) O. Shekhah, J. Liu, R. Fischer and C. Wöll, *Chem. Soc. Rev.*, 2011, **40**, 1081; (b) J. Yao and H. Wang, *Chem. Soc. Rev.*, 2014, **43**, 4470; (c) H. Furukawa, K. E. Cordova, M. O'Keeffe and O. M. Yaghi, *Science*, 2013, **341**, 1230444.
- 3 H. Bux, F. Liang, Y. Li, J. Cravillon, M. Wiebcke and J. Caro, *J. Am. Chem. Soc.*, 2009, **131**, 16000.
- 4 O. Shekhah, L. Fu, R. Sougrat, Y. Belmabkhout, A. J. Cairns, E. P. Giannelis and M. Eddaoudi, *Chem. Commun.*, 2012, **48**, 11434.
- 5 O. Shekhah and M. Eddaoudi, *Chem. Commun.*, 2013, **49**, 10079.
- 6 O. Shekhah, R. Swaidan, Y. Belmabkhout, M. Du Plessis, T. Jacobs, L. J. Barbour, I. Pinnau and M. Eddaoudi, *Chem. Commun.*, 2014, **50**, 2089.
- 7 S. Qiu, M. Xue and G. Zhu, *Chem. Soc. Rev.*, 2014, **43**, 6116.
- 8 A. Huang, H. Bux, F. Steinbach and J. Caro, *Angew. Chem.*, 2010, **122**, 5078.
- 9 A. Huang, W. Dou and J. Caro, *J. Am. Chem. Soc.*, 2010, **132**, 15562.
- 10 A. Huang, Y. Chen, N. Wang, Z. Hu, J. Jiang and J. Caro, *Chem. Commun.*, 2012, **48**, 10981.
- 11 Q. Liu, N. Wang, J. r. Caro and A. Huang, *J. Am. Chem. Soc.*, 2013, **135**, 17679.
- 12 N. Wang, Y. Liu, Z. Qiao, L. Diestel, J. Zhou, A. Huang and J. Caro, *J. Mater. Chem. A*, 2015, **3**, 4722.
- 13 Y. S. Li, H. Bux, A. Feldhoff, G. L. Li, W. S. Yang and J. Caro, *Adv. Mater.*, 2010, **22**, 3322.
- 14 T. Ben, C. Lu, C. Pei, S. Xu and S. Qiu, *Chem.–Eur. J.*, 2012, **18**, 10250.
- 15 J. Fu, S. Das, G. Xing, T. Ben, V. Valtchev and S. Qiu, *J. Am. Chem. Soc.*, 2016, **138**, 7673.
- 16 Z. Kang, M. Xue, L. Fan, L. Huang, L. Guo, G. Wei, B. Chen and S. Qiu, *Energy Environ. Sci.*, 2014, **7**, 4053.
- 17 H. Guo, G. Zhu, I. J. Hewitt and S. Qiu, *J. Am. Chem. Soc.*, 2009, **131**, 1646.
- 18 P. Neelakanda, E. Barankova and K.-V. Peinemann, *Microporous Mesoporous Mater.*, 2016, **220**, 215.
- 19 X. Zhang, Y. Liu, S. Li, L. Kong, H. Liu, Y. Li, W. Han, K. L. Yeung, W. Zhu and W. Yang, *Chem. Mater.*, 2014, **26**, 1975.
- 20 (a) Y. Liu, N. Wang, J. H. Pan, F. Steinbach and J. Caro, *J. Am. Chem. Soc.*, 2014, **136**, 14353; (b) Y. Liu, J. H. Pan, N. Wang, F. Steinbach, X. Liu and J. Caro, *Angew. Chem.*, 2015, **127**, 3071.
- 21 X. Zhang, Y. Liu, L. Kong, H. Liu, J. Qiu, W. Han, L.-T. Weng, K. L. Yeung and W. Zhu, *J. Mater. Chem. A*, 2013, **1**, 10635.
- 22 (a) G. H. A. Therese and P. V. Kamath, *Chem. Mater.*, 2000, **12**, 1195; (b) L.-X. Ding, A.-L. Wang, G.-R. Li, Z.-Q. Liu, W.-X. Zhao, C.-Y. Su and Y.-X. Tong, *J. Am. Chem. Soc.*, 2012, **134**, 5730.
- 23 D. Fairen-Jimenez, S. Moggach, M. Wharmby, P. Wright, S. Parsons and T. Duren, *J. Am. Chem. Soc.*, 2011, **133**, 8900.
- 24 (a) J. Yao, D. Dong, D. Li, L. He, G. Xu and H. Wang, *Chem. Commun.*, 2011, **47**, 2559; (b) K. Tao, L. Cao, Y. Lin, C. Kong and L. Chen, *J. Mater. Chem. A*, 2013, **1**, 13046; (c) J. Li, W. Cao, Y. Mao, Y. Ying, L. Sun and X. Peng, *CrystEngComm*, 2014, **16**, 9788; (d) Y. Hu, J. Wei, Y. Liang, H. Zhang, X. Zhang, W. Shen and H. Wang, *Angew. Chem., Int. Ed.*, 2016, **55**, 2048.